

CHROM. 11,747

## INSTABILITY AND NON-LINEARITY OF THE pH GRADIENT FORMED IN ISOELECTRIC FOCUSING

A. MUREL\*, I. KIRJANEN\*\* and O. KIRRET

*Institute of Chemistry of the Academy of Sciences of the Estonian S.S.R., 14 Akadeemia tee, 200026 Tallinn (U.S.S.R.)*

(First received April 26th, 1978; revised manuscript received January 11th, 1979)

---

### SUMMARY

A model of the pH gradient formed by two ampholytes is suggested. The calculations reveal that a step pH gradient can exist. The plateau effect and the influence of the pH and/or concentration of the electrolytes on the decay of the pH gradient are explained. By analogy with an electron cloud on the cathode of a thermionic valve, a proton cloud at the anodic end of anticonvective media is suggested for explaining the cathodic drift.

---

### INTRODUCTION

Isoelectric focusing (IEF) is a method for the separation and concentration of amphoteric molecules in a natural pH gradient, at a pH zone corresponding to their isoelectric points (*pI*). Instability of the pH gradient formed by carrier ampholytes in anticonvective media in an electric field remains one of the problems in isoelectric focusing. This instability is accompanied by relative displacement of the protein and carrier ampholyte bands, and by two-directional movement of carrier ampholytes from anticonvective media into the electrolyte reservoirs, predominantly into the catholyte (cathodic drift). These instabilities are of limited practical interest because they become noticeable only after the time usually employed for the fractionation of proteins. However, decay of the pH gradient is incompatible with the fundamental interpretation of isoelectric focusing as a static phenomenon.

It was found<sup>1,2</sup> that the cathodic drift could be decreased (a) by an increase in the carrier ampholyte concentration, (b) by a decrease in the field strength, (c) by an increase in the viscosity of the anticonvective media and (d) by equalization of the anolyte pH with the *pI* of the most acidic carrier ampholyte. It was noted that the pH of catholyte has little, if any, effect on the cathodic drift. However, it was recently found<sup>3</sup> that with a weak anolyte [reduced pH (and *pI*) difference between the anolyte and the most acidic carrier ampholyte] and a strong catholyte, the cathodic drift is

---

\* To whom correspondence should be addressed.

\*\* Responsible for computer calculations.

not only stopped, but the direction of the drift is even reversed and becomes anodic.

Several hypotheses have been advanced to explain the decay of the pH gradient<sup>2</sup>. As all of the mechanisms of the pH gradient instability have been reviewed by Rilbe<sup>4</sup>, we shall mention only a few of them here.

The present concept that decay of the pH gradient involves electrophoresis of partially charged carrier ampholytes is confirmed by the results of Cann and Stimpson<sup>5,6</sup>. However, this mechanism does not serve to explain the predominant movement of carrier ampholytes into the catholyte reservoir.

The cathodic direction of drift could be explained on the basis of the electro-osmotic hypothesis<sup>4</sup>, according to which the cathodic drift is produced by carboxylate charges on the gel. Nguyen *et al.*<sup>3</sup> found this mechanism to be incompatible with the reversibility of the drift direction.

The carrier ampholyte distribution coincides with the pH gradient and changes continuously during IEF. The electric field causes redistribution of the carrier ampholyte in the anticonvective media with no clear possibility of recognizing the pH gradient formation, "equilibrium" and decay<sup>7</sup>. As these three stages of the "life" of the pH gradient appear to be subjected to a uniform mechanism, it could be expected that the mechanism of the pH gradient could be evaluated through a consideration of the "equilibrium" (*i.e.*, steady state).

The steady state has its own unexplained problems. According to the law of pH monotony<sup>8</sup>, focused ampholytes must have continuous interdigitation among their peaks. Brown *et al.*<sup>9</sup> found that [<sup>14</sup>C]histidine (His) has another distribution profile in IEF using polyacrylamide gel, namely a plateau distributed over 40% of the column length. Alternatively, if we assume a linear pH gradient, as usual, one would be faced with the finding that His is isoelectric over a range of *ca.* 3 pH units. Righetti<sup>10</sup> considered that this fact is not true; as His is a "good" carrier ampholyte<sup>11</sup>, he assumed that the square-wave distribution typical of isotachopheresis (ITP) is incompatible with IEF, and is probably a "non-focusing" effect.

Nevertheless, such a distribution of His and some other amino acids, causing flattening at pH values near their *pI*, has already been employed in order to obtain shallow pH gradients<sup>12</sup>.

In this work we offer an explanation of the non-linearity and decay of the pH gradient.

## THEORETICAL

In the theory of IEF developed by Svensson<sup>13</sup>, a pH gradient is characterized as being created by a concentration distribution of carrier ampholytes represented by a series of bell-shaped curves, one for each ampholyte. This model is based on a logical conclusion because of the impossibility of formulating a simple mathematical general solution of a system of mutually dependent differential equations.

Svensson considered the behaviour of one of the ampholytes in the linear pH gradient already formed. He inferred a differential equation which can be written as follows:

$$CUE = D \cdot \frac{dC}{dx} \quad (1)$$

where

- $C$  = concentration of component and ion constituent;
- $U$  = electric mobility of ion constituent except  $H^+$  and  $OH^-$ , with a positive sign for cationic and a negative sign for anionic migration;
- $E$  = electric field strength;
- $D$  = diffusion coefficient of component;
- $x$  = coordinate along the direction of current.

Assuming a constant conductivity and constant conductivity and constant pH gradient, Svensson developed the following equation for a focused zone:

$$x_i = \left(\frac{D}{Ep}\right)^{\frac{1}{2}} \quad p = \frac{dU}{dx} = \frac{dU}{dpH} \cdot \frac{dpH}{dx} \quad (2)$$

where  $x_i$  denotes the width of the Gaussian distribution of the focused ampholyte measured from the top of the bell-shaped curve to the inflexion point.

Better separations could be achieved, as can be seen from eqn. 2 by decreasing  $D$  (i.e., by increasing the viscosity of anticonvective media), or by increasing the field strength  $E$  or employing narrow pH gradients.

The questions of interest, however, are the following: has the pH gradient really been created by a large number of ampholytes, each having a bell-shaped concentration distribution?; is it really linear?; if not, then what is its microstructure?

Let us consider a system of  $n$  ( $n \geq 2$ ) ampholytes, each ampholyte  $i$  having the same  $D$ , the same  $dU/dpH$  and the same concentration. Let us assume a constant, sufficiently small value of  $pI_i - pI_{i+1}$ ; the buffering capacity is the same and strong enough for each ampholyte in the region of its  $pI$ .

Then, if we take a mixture of carrier ampholytes  $i$  and  $i + 1$  in different proportions, the pH of such a mixture will change linearly from  $pH = pI_i$  to  $pH = pI_{i+1}$ , as can be seen in Fig. 1. The charge  $Z$  of ampholyte  $i$  will change in the same manner, i.e., from 0 to  $Z_i^*$ , and the mobility  $U_i$  from 0 to  $U_i^*$ . One can then write:

$$\frac{U_i^* - U_i}{U_i} = \frac{C_i}{C_{i+1}}$$

where  $C_i$  is the concentration of ampholyte  $i$  in the mixture. Hence

$$U_i = U_i^* \cdot \frac{C_{i+1}}{C_i + C_{i+1}} \quad (3)$$

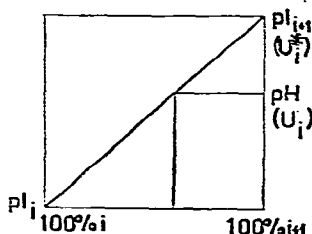


Fig. 1. Dependence of pH (and  $U$ ) on the components in mixtures.

Let us also assume, as was done by Svensson<sup>13</sup>, that the field strength  $E$  is constant throughout the whole focusing system (note that we do not consider an *a priori* linear pH gradient). Suppose that we have subjected this system of two ampholytes to IEF in anticonvective media (or, which is the same thing, consider a sufficiently small section of the created pH gradient containing only ampholytes  $i$  and  $i + 1$ ).

Then one obtains the following equation of the equilibrium between diffusional and electrical mass transport for ampholytes  $i$  and  $i + 1$ , and from eqn. 3:

$$\begin{aligned} -D_i \cdot \frac{dC_i}{dx} &= EU_i C_i = EU_i^* \cdot \frac{C_i C_{i+1}}{C_i + C_{i+1}} \\ D_{i+1} \cdot \frac{dC_i}{dx} &= EU_{i+1}^* \cdot \frac{C_i C_{i+1}}{C_i + C_{i+1}} \end{aligned} \quad (4)$$

where  $x$  is still the coordinate along the direction of current, increasing towards the cathode. The negative sign before  $dC_i/dx$  means that diffusional mass transport is negative,  $C_i$  decreasing with increasing  $x$ .

It is more convenient to use the equation system (4) in the form

$$\begin{aligned} -M_i \cdot \frac{dC_i}{dx} &= \frac{C_i C_{i+1}}{C_i + C_{i+1}} \\ M_{i+1} \cdot \frac{dC_{i+1}}{dx} &= \frac{C_i C_{i+1}}{C_i + C_{i+1}} \end{aligned} \quad (4a)$$

where  $M$  is the ratio  $D/EU^*$ .

Computations were made on a Videoton 1010B computer.  $\Delta x = 0.1$  was the transport part of the calculations (see Appendix). Initial conditions are given in Table I. The calculations illustrated by the results in Figs. 2–8 are represented by pairs of distribution curves, each pair for a certain initial condition; the curve for component  $i$  decreases and that for component  $i + 1$  increases with increase in  $x$ .

These curves help us to understand the qualitative picture of ampholyte focusing.

## RESULTS AND DISCUSSION

### (A) pH gradient structure

(i) *Symmetry of distribution curves.* The distribution curves (curves A–G, in the figures) are symmetrical for a system of two ampholytes with  $M_i = M_{i+1}$  (ampholytes with “identical properties”). The sum of ampholyte concentrations is constant\* at every point of the anticonvective media,  $C_i$  and  $C_{i+1}$  being nowhere equal to zero (see Appendix).

(ii) *Influence of  $M$  on the separation.* As could be derived from eqn. 4a, an  $n$ -fold increase in both  $M_i$  and  $M_{i+1}$  causes an  $n$ -fold increase in the abscissa scale (Figs. 2 and 3); the greater is  $M$  (*i.e.*, the greater the viscosity and/or the field strength), the better is the separation.

TABLE I  
INITIAL CONDITIONS FOR COMPUTATION OF EQN. 4

$D_i$	$D_{i+1}$	$EU_i$	$EU_{i+1}$	Value of $C$ at $x = 0$		Curve pair	Fig. No.
				$C_i^0$	$C_{i+1}^0$		
1	1	20	20	1.00001	0.00011	A	2,3
1	1	10	10	1.00001	0.00011	B	2,3,4
2	2	20	20	1.00001	0.00011		
5	5	50	50	1.00001	0.00011		
1	1	7.5	7.5	1.00001	0.00011	C	2,7
1	1	5	5	1.00001	0.00011	D	3
1	1	1	1	1.00001	0.00011	E	3
1	1	10	10	2.00002	0.00022	F	4
1	1	10	10	5.00005	0.00055	G	4
1	1	5	10	1.00001	0.00011	I	5,6
1	1	5	20	1.00001	0.00011	J	5
1	1	5	50	1.00001	0.00011	K	5
1	1	10	20	1.00001	0.00011	H	6
1	1	7.5	7.5	0.80001	0.20011	C	7a
				0.50001	0.50011		7b
				0.20001	0.80011		7c
1	1	10	20	0.98001	0.02011	H	8
1	1	5	10	0.98001	0.02011	I	8

(iii) *Influence of  $C_i^0$  and  $C_{i+1}^0$ .* An increase in both  $C_i^0$  and  $C_{i+1}^0$  leads to a proportional increase in the ordinate scale, the inflexion points being at the same points on the abscissa  $x$  (Fig. 4). This means that the slope of the pH gradient does not change when the carrier ampholyte concentration changes.

(iv) *Plateau effect.* As one can conclude from Figs. 2 and 3, the ampholyte concentration, under certain conditions, is represented not by a series of bell-shaped curves<sup>13</sup> but by a series of plateaux, which are Gaussian-shaped at their ends.

As the slope of the curve for component  $i + 1$  coincides with pH growth, the pH gradient may also have plateaux. If only one of the ampholytes has a sufficiently high concentration (for instance, component  $i + 1$  in curve A, Fig. 2), then there will

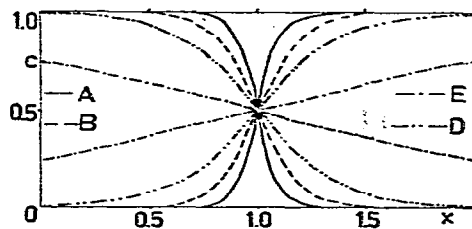
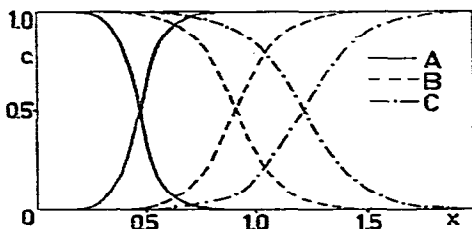


Fig. 2. Influence of  $M = D/EU^*$  on the distribution of ampholytes. Curve pair A,  $M = 1/20$ ; B,  $M = 1/10$ ; C,  $M = 1/7.5$ .  $C_i^0$  and  $C_{i+1}^0$  are the same for all curve pairs.

Fig. 3. Influence of  $M$  on the ampholyte distribution. All curve pairs have been displaced in order to combine the inflexion points in the middle of graph. The sum  $C_i + C_{i+1}$  is the same for all curve pairs. Curve pair A,  $M = 1/20$ , B,  $M = 1/10$ ; D,  $M = 1/5$ ; E,  $M = 1$ .

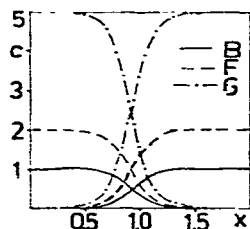


Fig. 4. Influence of  $C_i^0$  and  $C_{i+1}^0$  on ampholyte distribution. Curve pair B,  $C_i^0 = 1.00001$ ,  $C_{i+1}^0 = 0.00011$ ; F,  $C_i^0 = 2.00002$ ,  $C_{i+1}^0 = 0.00022$ ; G,  $C_i^0 = 5.00005$ ,  $C_{i+1}^0 = 0.00055$ .  $M$  is the same for all curve pairs ( $M = 1/10$ ).

be only one plateau (a zone of "pure water" or of a "separator"<sup>12</sup>), and, *vice versa*, the greater the number of carrier ampholytes, the smaller will be the partial concentration of the individual ampholyte in the mixture, the more even is the pH gradient.

Every carrier ampholyte mixture containing a limited number of components should have, at a certain  $M$ , a step pH gradient. For instance, such plateaux can be observed in the pH gradient formed by a poor mixture of ampholytes (Figs. 3 and 4 in ref. 14).

Nevertheless, a poor ampholyte mixture can also form an even pH gradient at a certain value of  $M$  [see section (ii) and Fig. 3, *cf.* curves E to A].

(v) *Micro-structure of pH gradients.* Let us consider a step pH gradient formed by 7000 carrier ampholytes with *pI* values from 3 to 10; the gel length is 20 cm. There would be pH steps of 0.01 pH unit in 0.028 cm; it is virtually impossible to measure such small steps.

In fact, pH is usually measured after the electric field has been switched off. In the absence of an electric field, the decay of the microstructure of the pH gradient immediately begins to be due to diffusion. A higher viscosity of anticonvective media will prolong the "life" of the microstructure.

While working with coloured ampholytes<sup>15</sup> (synthesized according to Vinogradov *et al.*<sup>16</sup>, but not purified), we observed clearly pronounced zones of different width with a homogeneous colour throughout (plateaux). After the potential had been switched off the zones remained visible for 5–15 min in Sephadex G-100 gel, and then disappeared owing to diffusion. The pH gradient is stable for a longer period after the potential has been switched off. This fact could be explained by the similarity of ampholytes. The diffusion from both sides to the examined point occurs at the same rate and the ampholytes neutralize one another, the initial pH remaining the same. The destruction of the pH gradient was faster from the ends of the gel.

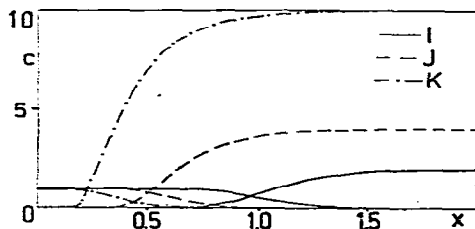


Fig. 5. Ampholytes with "different properties": influence of  $M_{i+1}$  on distribution curves. Curve pair I,  $M_{i+1} = 1/10$ ; J,  $M_{i+1} = 1/20$ ; K,  $M_{i+1} = 1/50$ .  $C_{i+1}^0$  and  $M_i = 1/5$  are the same for all curve pairs.

(vi) *System of ampholytes with different properties.* Now, let us assume that we have two ampholytes with different properties ( $M_i \neq M_{i+1}$ ) such as different molecular weights or configurations ( $D_i \neq D_{i+1}$ ), and/or different mobilities ( $U_i^* \neq U_{i+1}^*$ ). The results of calculations for such a system are represented by distribution curves H-K in the figures.

As can be concluded from the distribution of ampholytes represented in Fig. 5, the greater the difference between  $M_i$  and  $M_{i+1}$ , the greater is the difference between  $C_i^{\max}$  and  $C_{i+1}^{\max}$ :

$$\frac{C_i^{\max}}{C_{i+1}^{\max}} = \frac{M_{i+1}}{M_i} = \frac{D_{i+1}}{D_i} \cdot \frac{U_i^*}{U_{i+1}^*} \quad (5)$$

where  $C_i^{\max} = \lim_{x \rightarrow -\infty} C_i$ ,  $C_{i+1}^{\max} = \lim_{x \rightarrow \infty} C_{i+1}$ .

It is clear from Fig. 6 that the behaviour of the distribution curves has the same dependence on  $M$  as is the case with ampholytes with identical properties [see sections (ii) and (iii)].

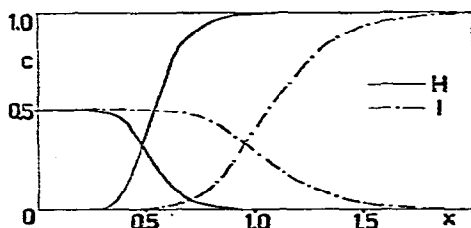


Fig. 6. Ampholytes with "different properties": influence of  $M_i$  and  $M_{i+1}$  on distribution curves. Curve pair I,  $M_i/M_{i+1} = 10/5 = 2$ ; H,  $M_i/M_{i+1} = 20/10 = 2$ .  $C^*$  and  $C_{i+1}^*$  are the same for all curve pairs.

According to eqn. 5 the proteins could be concentrated by IEF to a much greater extent than the relatively low-molecular-weight carrier ampholytes (the diffusional coefficient of a protein is much lower than that of a carrier ampholyte). However, there is an upper concentration limit dictated by eqn. 5 (if we do not consider possible precipitation of proteins at their  $pI$  values). As with "identical" ampholytes [see section (iv)], the protein distribution curve can also have a plateau. Hence, there is no load limit for proteins subjected to IEF: even at very low relative concentrations of carrier ampholytes they will separate proteins from one another (in the absence of isoelectric precipitation and a low conductivity of precipitated zones).

(vii) *Law of pH monotony.* Suppose that we have applied two ampholytes at opposite ends of the gel. Let us consider water to be an absolute insulator (otherwise we would have to consider water to be an ampholyte). Then there will be no conductivity in this system, no potential, and all mass transport will be due to diffusion. Contact between the ampholytes would appear and the ampholytes would receive charges in the zone of contact and rearrange in the gel by diffusional and electric forces according to their  $pI$  values to satisfy eqn. 4 [see section (i)]. This is a very simple explanation of the law of pH monotony<sup>8</sup>, and we do not understand why Haglund<sup>17</sup> considered that this law had never been proved theoretically.

*(B) pH gradient decay*

*(viii) System of two ampholytes, one being an electrolyte.* Let us suppose now that the point  $x = 0$  on the graphs represents the boundary between an anticonvective medium ( $x > 0$ ) and electrolyte solution ( $x < 0$ ), with component  $i$  being an electrolyte\*. Suppose that we have an electrolyte reservoir of infinite volume with electrolyte concentration  $C = C_i^0$ , the gel volume being restricted. Let us suppose also that the electrolyte solution is vigorously stirred so that the concentrations of all substances present in the electrolyte reservoir are equal throughout the volume. Then some molecules of ampholyte  $i + 1$ , once having been washed out, will remain in the electrolyte reservoir with a zero probability of being brought back into the anticonvective medium.

*(ix) Influence of  $C_i^0$  and  $C_{i+1}^0$  on the diffusion of component  $i + 1$  out of the gel.* The distribution curves of components dependent on the electrolyte concentration  $C_i^0$  can be obtained. The curves are represented in Fig. 7.

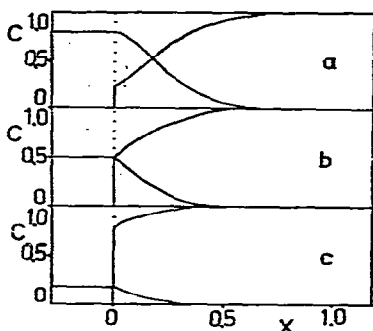


Fig. 7. Influence of electrolyte concentration  $C_i^0$  on  $C_{i+1}^0$ , i.e., on the rate of diffusion,  $V$ , of component  $i + 1$  out of gel. First approximation:  $V = -dC_{i+1}/dt = D_{i+1} \cdot C_{i+1}^0/dx$ .  $M$  is the same for all curve pairs ( $M = 1/7.5$ ). (a)  $C_i^0 = 0.80001$ ,  $C_{i+1}^0 = 0.20011$ ; (b)  $C_i^0 = 0.50001$ ,  $C_{i+1}^0 = 0.50011$ ; (c)  $C_i^0 = 0.20001$ ,  $C_{i+1}^0 = 0.80011$ .

Let us assume to a first approximation that the rate of diffusion of the terminal ampholyte out of the anticonvective medium is directly proportional to  $C_{i+1}^0$ . Hence, the greater the electrolyte concentration  $C_i^0$ , the smaller is  $C_{i+1}^0$  (cf., Fig. 7a-c) and the lower is the rate of diffusion of ampholyte  $i + 1$  into this electrolyte.

*(x) Influence of electrolyte pH on the pH gradient decay.* The ampholytes receive charges from their contact with electrolytes. The greater is the concentration of the electrolyte, the greater are the charges received (Fig. 1). As the terminal ampholytes are charged by  $H^+$  and  $OH^-$  ions of anolyte and catholyte, respectively, we find that  $C_i$  describes the  $H^+$  ( $OH^-$ ) concentration. With this conclusion we can explain why the cathodic drift was lowered (and even reversed to anodic) when lysine was replaced with arginine of the same molar concentration<sup>3</sup>.  $C_i^0$  for 0.01 M arginine ( $pH_{25^\circ} = 10.3$ ) is  $10^{0.8} = 6.3$ -fold greater than  $C_i^0$  for 0.01 M lysine ( $pH_{25^\circ} = 9.5$ ) (cf. Fig. 7).

*(xi) Influence of the  $C_{i+1}$  distribution profile on the pH gradient decay velocity.* The first approximation stating that the decay of the pH gradient depends only on the value of  $C_{i+1}^0$  is not completely correct, because the diffusion of component  $i + 1$

\* The real behaviour of components near the phase boundary is much more complicated.



depends on the  $C_{i+1}$  profile near the boundary of the anticonvective medium. It is obvious now that the rate of decay of the pH gradient will be diminished with increase in  $M$ , for instance, with decrease in the electric field strength, or with an increase in the viscosity of the anticonvective media (Fig. 8, curve H to I). This conclusion is confirmed by the results of Chrambach *et al.*<sup>2</sup>.

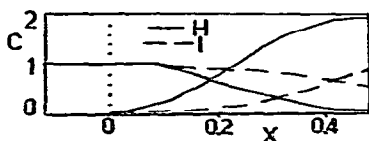


Fig. 8. Influence of  $M$  on the  $C_{i+1}$  profile near the gel boundary. Electrolyte concentration  $C_i^0$  and  $C_{i+1}^0$  are the same for both curve pairs. It is expected here that the diffusional mass flow through a shallow "concentration corridor" (curve I) out of gel will be slower than with a broad one (curve H).

(xii) *Influence of the difference between the pI (and pH) values of the terminal ampholyte and electrolyte.* Let us suppose that after a certain period of IEF the first terminal ampholyte has completely diffused out of anticonvective medium into the electrolyte chamber. Now the second ampholyte will be brought into contact with the electrolyte, and it will be charged on contact to a slightly greater extent than in the case of the first ampholyte, owing to the greater difference between the electrolyte pH and its pI value. The greater the charge (and mobility  $U^*$ ) and the smaller is  $M$ , the faster is the rate of transport of ampholytes out of the gel (see Fig. 8).

(xiii) *Electrolyte pressure upon ampholytes.* As can be seen from Fig. 7, an increase in  $C_i^0$  causes a shift of carrier ampholytes into the depth of the anticonvective medium. After a certain concentration  $C_i^0$ , which is an inflexion point on the  $C_i$  curve, the pressure upon the ampholytes increases very rapidly with increase in  $C_i^0$  (compare Fig. 7a with Fig. 2, curve C).

Suppose that we have an equilibrated focusing system with a symmetrical and negligible value of ampholyte loss into the electrolyte reservoirs. Let us now suppose that we have increased the anolyte concentration  $C_i^0$ , *i.e.*, reduced the pH of the anolyte. Ampholytes would have to move towards the cathode. Then a smaller volume of gel would be left for carrier ampholytes, causing an increase in their concentration, until a level controlled by eqn. 4 is satisfied. However, the increase in the ampholyte concentration will lead to more rapid diffusion into the catholyte reservoir [see section (ix)]. This is why Nguyen and Chrambach<sup>1</sup> increased the cathodic drift by reducing the anolyte pH.

(xiv) *Hypothesis of a "proton cloud".* We now suggest a hypothesis to explain the predominant cathodic direction of the decay of the pH gradient. We think that the main probable reason for this may be the difference in the nature of  $\text{OH}^-$  and  $\text{H}^+$  ( $\text{H}_3\text{O}^+$ ) ions, *viz.*, the great difference in their sizes. We believe that by analogy with the electronic cloud on the cathode of a thermionic valve, a proton cloud at the anodic end of the anticonvective medium could exist. From the theory of the diffusion of electrolytes, we know that the ions with greater  $D$  can diffuse faster and move ahead, causing the emergence of a potential  $E$ . At the steady state, this distance of outstripping is kept constant, depending on  $E$  and  $D_i$ . This means that the  $\text{H}^+$  ions of the anolyte and the  $\text{OH}^-$  ions of the catholyte penetrate deeper into the gel than would be expected from the distribution curves. Under the same conditions of IEF

experiment,  $H^+$  ions are found much deeper in the gel than  $OH^-$  ions, protecting the anodic end from the rapid diffusion of ampholytes out of the anticonvective medium (compare Figs. 7a and 7c).

The main reason for the decay of the pH gradient [see section (xiii)] appears to be the pressure of the electrolyte. The electrophoresis of partially charged terminal constituents and electroendosmosis can accelerate the decay.

#### APPENDIX

The equation system 4 was integrated by the Runge-Kutta method using a Videoton 1010B computer.

Boundary points

$$C_i^0 = 1, C_{i+1}^0 = 0$$

and

$$C_i^0 = 0, C_{i+1}^0 = 1$$

are singular and there is no solution for eqn. 4 in these points.

The text of the program in Fortran is as follows:

```

SUBROUTINE INTEG(DI,DI1,UI,UI1,E,X0,XMAX,H,Y0,YY,S)
CCCCC
DI = DIFFUSIONAL COEFFICIENT OF I-COMPONENT
DI1 = DIFFUSIONAL COEFFICIENT OF I+1-COMPONENT
UI = MOBILITY OF I-COMPONENT FROM EQ.(3)
UI1 = MOBILITY OF I+1-COMPONENT FROM EQ.(3)
E = ELECTRIC FIELD STRENGTH
X0 = INITIAL VALUE OF COORDINATE ALONG THE DIRECTION OF CURRENT
XMAX = FINAL VALUE OF COORDINATE ALONG THE DIRECTION OF CURRENT
H = STEP OF INTEGRATION
Y0 = CONCENTRATIONS OF COMPONENTS AT X0
YY = CONCENTRATIONS OF COMPONENTS ALONG DIRECTION OF CURRENT
S = SUM OF CONCENTRATIONS OF COMPONENTS ALONG DIRECTION OF CURRENT
N = NUMBER OF EQUATIONS.
DIMENSION V1(1),V2(1),Y0(1),Y1(1),F(1),YY(1),S(1)
N1=FIX(ABS((X0-XMAX)/H))
N2=1
DO 1 I=1,N
  Y1(I)=Y0(I)
  L1=1
  GOTO 8
10 DO 2 I=1,N
  V1(I)=H*F(I)
  Y1(I)=Y0(I)+V1(I)/2.0
  V2(I)=V1(I)/6.0
  X0=X0+H/2.0
  L1=2
  GOTO 8
11 DO 3 I=1,N
  V1(I)=H*F(I)
  Y1(I)=Y0(I)+V1(I)/2.0
  V2(I)=V2(I)+V1(I)/3.0
  L1=3
  GOTO 8
12 DO 4 I=1,N
  V1(I)=H*F(I)
  Y1(I)=Y0(I)+V1(I)
  V2(I)=V2(I)+V1(I)/3.0
  X0=X0+H/2.0
  L1=4
  GOTO 8
13 DO 5 I=1,N
  V1(I)=H*F(I)
  V2(I)=V2(I)+V1(I)/6.0
  Y0(I)=Y0(I)+V2(I)
  DO 9 I=1,N
  YY((N2-1)*2+I)=Y0(I)
  S(N2)=Y0(1)+Y0(2)
  N2=N2+1
  IF (N2=N1) 6,6,7
7 STOP
8 AB1=Y1(1)+Y1(2)
  AB2=Y1(1)*Y1(2)
  F(1)=E*UI*AB2/(DI*AB1)
  F(2)=E*UI1*AB2/(DI1*AB1)
  GOTO (10,11,12,13),L1
RETURN

```

## REFERENCES

- 1 N. Y. Nguyen and A. Chrambach, *Anal. Biochem.*, 82 (1977) 226.
- 2 A. Chrambach, P. Doerr, G. R. Finlayson, L. E. M. Miles, R. Sherins and D. Rodbard, *Ann. N.Y. Acad. Sci.*, 209 (1973) 44.
- 3 N. Y. Nguyen, A. G. McCormik and A. Chrambach, *Anal. Biochem.*, 88 (1978) 186.
- 4 H. Rilbe, in B. J. Radola and D. Graesslin (Editors), *Electrofocusing and Isotachopheresis*, De Gruyter, Berlin, New York, 1976, p. 35.
- 5 J. R. Cann and D. I. Stimpson, *Biophys. Chem.*, 7 (1977) 103.
- 6 D. I. Stimpson and J. R. Cann, *Biophys. Chem.*, 7 (1977) 115.
- 7 A. Chrambach and N. Y. Nguyen, in B. J. Radola and D. Graesslin (Editors), *Electrofocusing and Isotachopheresis*, De Gruyter, Berlin, New York, 1976, p. 51.
- 8 H. Svensson, *Protides Biol. Fluids, Proc. Colloq.*, 15 (1967) 515.
- 9 R. K. Brown, M. L. Caspers, J. M. Lull, S. N. Vinogradov, K. Felgenhauer and M. Nekić, *J. Chromatogr.*, 131 (1977) 2223.
- 10 P. G. Righetti, *J. Chromatogr.*, 138 (1977) 213.
- 11 H. Svensson, *Acta Chem. Scand.*, 16 (1962) 456.
- 12 M. L. Caspers, Y. Posey and R. K. Brown, *Anal. Biochem.*, 79 (1977) 166.
- 13 H. Svensson, *Acta Chem. Scand.*, 15 (1961) 325.
- 14 O. Vesterberg, *Acta Chem. Scand.*, 23 (1969) 2653.
- 15 A. Murel, in preparation.
- 16 S. N. Vinogradov, S. Lowendron, M. R. Andonian, J. Bagshaw, K. Felgenhauer and S. J. Pak, *Biochim. Biophys. Acta*, 54 (1973) 501.
- 17 H. Haglund, *Methods Biochem. Anal.*, 19 (1970) 16.